THE JOURNAL OF PHYSICAL CHEMISTRY B

pubs.acs.org/JPCB Article

Compression and Stretching of Single DNA Molecules under Channel Confinement

Tomáš Bleha and Peter Cifra*

Cite This: J. Phys. Chem. B 2020, 124, 1691−1702 Read Online

ACCESS | Metrics & More | Article Recommendations | Supporting Information

ABSTRACT: We study the compression and extension response of single dsDNA (double-stranded DNA) molecules confined in cylindrical channels by means of Monte Carlo simulations. The elastic response of micrometer-sized DNA to the external force acting through the chain ends or through the piston is markedly affected by the size of the channel. The interpretation of the force (f)−displacement (R) functions under quasi-one-dimensional confinement is facilitated by resolving the overall change of displacement ΔR into the confinement contribution ΔR_D and the force contribution ΔR_f. The external stretching of confined DNA results in a characteristic pattern of f−R functions involving their shift to the larger extensions due to the channel-induced pre-stretching ΔR_D. A smooth end-chain compression into loop-like conformations observed in moderately confined DNA can be accounted for by the relationship valid for a Gaussian chain in bulk. In narrow channels, the considerably pre-stretched DNA molecules abruptly buckle on compression by the backfolding into hairpins. On the contrary, the piston compression of DNA is characterized by a gradual reduction of the chain span S and by smooth f−S functions in the whole spatial range from the 3d near to 1d limits. The observed discrepancy between the shape of the f−R and f−S functions from two compression methods can be important for designing nanopiston experiments of compaction and knotting of single DNA in nanochannels.

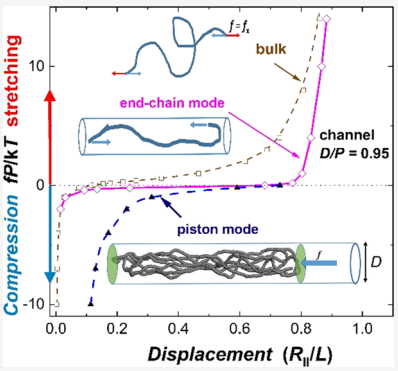

INTRODUCTION

The properties of semiflexible polymers such as the double-stranded (ds)DNA can be considerably modified by imposed constraints such as confinement or external force. It is well known that confinement and mechanical force share great similarities in their impact on polymer behavior.[1−3] The individual actions of confinement and force on the polymers are nowadays systematically described. A response of polymer chains to the applied force f is a classical topic of polymer statistical mechanics.[1] Advances in single-molecule techniques have made it possible to study single polymers under stretching force using atomic force microscopy and the optical and magnetic tweezers.[4,5] In the same way, the exploration of semiflexible molecules under confinement much gained from the experimental studies of DNA in nanofluidic devices.[6,7] On-chip platforms involving slit-like or tube-like channels allow precise manipulation of DNA molecules and the optical mapping of the genome.

The single-molecule experiments by pulling a polymer above its equilibrium size permit nowadays to establish at the molecular level the relationship between the force f and the chain end-to-end displacement R. The elastic response of semiflexible polymers is most often rationalized by the wormlike chain (WLC) model.[8] In the WLC model, a macromolecule is viewed as a thin continuous inextensible filament of flexural rigidity (bending stiffness) B and the contour length L. The persistence length $P = B/kT$ and the ratio L/P are employed to assess the stiffness of a macromolecule. The moderately stiff polymers such as micrometer-sized DNA are characterized by L/P in tenths or hundreds. A closed-form relationship of Marko and Siggia (MS)[9] based on the WLC model represents well the f−R curves from single-molecule measurements of DNA at moderate and large tensile forces. Its shortcoming at weak tensile forces was elucidated[10] by the disparity (the arithmetic vs the quadratic averages) in the quantities used to measure the chain size. In contrast to pulling, the measurement of the compression response of single semiflexible polymers is much less developed due to the lack of available tools. As an alternative, the compression functions f−R of DNA-like molecules from the constant force and the constant length simulations are available.[10]

In an analogy with the tensile force, confinement of a polymer into a channel of the diameter D also generates the longitudinal polymer extension. The corresponding quantity R_{II} is of primary interest in single DNA nanofluidic experiments. Two classic theories in the field due to de Gennes and Odijk[11,12] describe this effect. In the de Gennes

Received: December 16, 2019
Revised: February 5, 2020
Published: February 11, 2020

https://dx.doi.org/10.1021/acs.jpcb.9b11602
J. Phys. Chem. B 2020, 124, 1691−1702

blob scaling approach,[11] the polymer behavior is controlled by the competition of the dimension D with other length scales such as P and the chain diameter w. The classic de Gennes regime that arises in the channel sizes of several persistence lengths, the extension R_{II}, should scale proportionally to $D^{-0.7}$. The strongly confined polymers under a condition $D < P$ are described by the Odijk theory.[12] A DNA molecule is viewed in this theory as a sequence of rigid segments that deflect back and forth from the channel walls and generate a considerable chain extension. The existence of additional regimes in the experimentally relevant intermediate zone between the de Gennes and Odijk regimes is nowadays broadly accepted.[13]

In contrast to situations where macromolecules are only confined or only under force, our focus here is on DNA properties when both constraints are imposed. The simultaneous operation of confinement and the external force is encountered in, for example, gel electrophoresis where the polymers confined within gels are affected by the electric and hydrodynamic forces. Similarly, in nanofluidic devices, the "passive" extension of a DNA molecule induced by uniaxial confinement is combined with the "active" deformation of DNA by the mechanical, hydrodynamic, or electrical forces.[6,7] The theory and simulations were used to elucidate the combined action of both constraints for DNA-like molecules in slit-like pores.[14−18] The different scaling regimes of stretched semiflexible polymers confined in nanoslits have been described.[15,16] The force−extension relation for strongly confined wormlike chains in slits was formulated[17] by a modification of the MS equation. Furthermore, the tensile force−extension relation for DNA based on the effective dimensionality d_{eff} was deduced in the whole range of slit heights from 3d to 2d confinement.[18] The $f-R$ curves computed in the slits were shifted relative to the bulk state to larger extensions at equivalent forces.[17,18]

In nanochannels, the DNA behavior under combined D and f constraints is up to now elucidated only under specific restrictive conditions. Thus, the analytical relation $f-R$ was presented for DNA under strong channel confinement and strong tensile forces.[19,20] In the opposite limit of weak forces, the blob-scaling approach based on Flory-type expression of the free energy[13] was used to formulate the $f-R$ function for a flexible self-avoiding chain in a cylinder.[21,22] The function was later exploited in the simulation study of the bacterial chromosome.[23] However, 1d string of blobs in the de Gennes regime presumed in the formulation of the $f-R$ function[21] disregards the chain backfolding and, in addition, considers only the entropic deformation of a polymer. The elastic free energy profiles $A(R)$ and the related functions $f-R$ for the channel-confined DNA were reported[3] from simulations under the constant length at weak compression and stretching forces. The overall change of displacement ΔR of a DNA molecule under the combined effect of D and f constraints (relative to the stress-free size in bulk) was resolved into the contributions due to channel confinement, ΔR_D, and external force, ΔR_f. It was found that the chain extension by channel walls requires much larger free energy costs than the active extension by the external force.[3]

The present paper addresses the deformation of DNA molecules confined in cylindrical channels across the wide ranges of channel sizes and compressive and tensile forces. The force−displacement functions $f-R$ are obtained by Monte Carlo (MC) simulations based on the coarse-grained model of micrometer-sized DNA. The combined action of confinement and force is investigated by using (i) stretching and compression of confined molecules through the chain ends and (ii) compression of DNA by a piston moving in a nanochannel. The two deformation modes are relevant to the compression and expansion modes of confined DNA under mechanical, electric, or hydrodynamic forces in nanofluidic devices,[6,7,24,25] including the technique of movable nanopiston.[26−28] The stretching regime of the functions $f-R$ in confined DNA was found to be critically affected by the channel-induced pre-stretching term ΔR_D. In the compression regime, the force−displacement functions revealed gradual or abrupt compaction of a DNA molecule according to whether the end-to-end distance R_{II} or span S was used to express the chain displacement.

METHODOLOGY

The bead-spring discretized WLC model described in refs 29−31 was used to compute the mechanical deformation of confined dsDNA molecules. N partially fused spherical beads connected by effective bonds (characterized by the spring constant) are assumed in the model. Three contributions to the potential energy are considered: from bond stretching, from nonbonded pair interactions between beads U_{nb}, and from the bending of two consecutive effective bonds U_b. The bond stretching energy is described by the FENE potential in which the bond length can slightly vary around the preferred length l_o. The nonbonded interaction of two beads of the diameter w is modeled by the shifted and cut repulsive Morse potential. The diameter w slightly exceeds the effective bond length l because of the bead interpenetration. The penalty for the deviation of a chain from a straight rod is given as $U_b(\theta)/kT = (b/kT)(1 + \cos\theta)$, where θ is the valence angle between two consecutive bonds in the chain, and the parameter b is associated with the chain stiffness. Electrostatic interactions in a DNA molecule are implicitly included in the bending energy parameter b. The devised set of simulation parameters should represent the behavior of dsDNA at high salt concentrations.

The canonical MC simulations employing the Metropolis algorithm were carried out to sample equilibrium of the channel-confined conformations of DNA subject to the external force. The simulation protocol involves the chain updates by reptation and small random bead displacements in chain generation. One reptation move is combined with 10 bead displacements. Up to 2.10^7 MC steps including $\sim 10^{10}$ conformation updates were sampled in computing equilibrium chain properties. The constant DNA length of $N = 1000$ beads of the diameter $w = 2.5$ nm was considered in computations. The effective bond length $l = 2.3$ nm is slightly lower than diameter w due to bead interpenetration. The bond length l represents about 6.8 base pair (bp) in case 0.337 nm is taken for the average contribution of one bp to the helix rise. Hence, the DNA contour length $L = (N - 1)l = 2.3$ μm. The bending energy parameter b is related to the intrinsic persistence length P of the bulk DNA as $b/kT = P/l$. A selection of $b/kT = 20$ corresponds to $P = 46$ nm of DNA, that is, the persistence length amounts to 20 beads in the model. The assigned value of P is consistent with the experimental data for dsDNA in high ionic-strength buffers, where typically $P \approx 50$ nm.

The confinement of DNA molecules in cylindrical channels is modeled by using a soft-wall potential of the same form as that used for nonbonded repulsive interactions between chain

https://dx.doi.org/10.1021/acs.jpcb.9b11602
J. Phys. Chem. B 2020, 124, 1691−1702

beads. This potential acts between chain segments and walls separated by the cylinder diameter D^*. The accessible volume is thus reduced to an effective diameter $D = D^* - w$ due to wall repulsion. This assumption differs from the previously used[29−31] restriction of bead centers of a macromolecule to the diameter D^* that effectively increased the diameter of accessible volume by w. Many orders of the confinement strength are sampled in simulations, from very wide channels near the 3d limit of bulk DNA to the narrowest channel of $D \approx 10$ nm near the 1d limit. Periodic boundary conditions were applied along the long channel axis aligned with the x axis.

The average quantities were used in assessing the displacement of DNA molecules. The variations of the end-to-end distance under force and/or confinement are monitored by the quadratic average $R = \langle R^2 \rangle^{1/2}$, its longitudinal component along the x axis $R_{II} = \langle R^2_{II} \rangle^{1/2}$, and the arithmetic average $\langle x \rangle$ of the displacement vector in the direction of the x axis. Alternatively, the mean span S of a molecule is computed, given as the longest dimension of a polymer along the channel x axis: $S = \langle \max(x_i) - \min(x_j) \rangle$, where $i, j \in [1, N]$. The span is a common measure of DNA size in single-chain experiments under confinement. To evaluate the fluctuations around the equilibrium value of displacement, the variance $\sigma^2 = \langle R^2_{II} \rangle - \langle x \rangle^2$ was computed.

The mechanical deformation of confined DNA by the constant external force f oriented along with the x axis $f = f_x$ was explored by two simulation setups (Figure 1). The

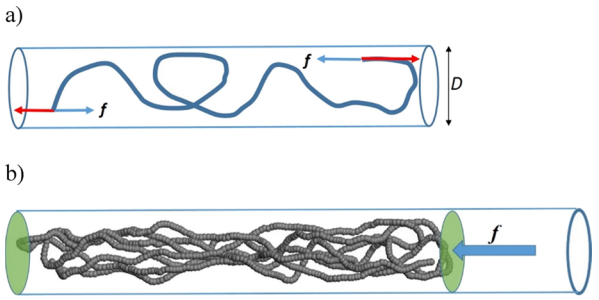

Figure 1. Two deformation mechanisms considered: (a) sketch of the tensile (red) and compressive (blue) force f acting on the chain ends and (b) the compressive force acting by piston method on the chain span (the snapshot from simulation for $D/P = 0.95$, $fP/kT = 10$).

negative force represents chain compression. In the first approach, the Metropolis algorithm was modified by the stretching/compression energy term added to the Boltzmann energy term for the attempted trial move. This extra term $dU = -f_x\, d|x|$ is given as the product of two scalar quantities: the force magnitude and the differential of the size of displacement R_{II} in the x-axis direction. Such a protocol in the constant-force simulations allows us to explore both the chain stretching and compression regimes[10] and thus to evaluate the full range of the function $f-R$ for the channel-confined DNA.

In the second approach (Figure 1b), only DNA compression under a movable piston is examined. The compression force f_x modifies the position of a mobile piston that closes the channel from one side, while the other side of the channel is closed by a fixed wall. Both the fixed wall and the piston interact with a chain in the same way as the channel walls described above. The distance of piston from the fixed wall is identical to the chain span S along the channel. The extra term added to the Metropolis algorithm, in this case, is $dU = -f_x\, d|x_p|$, where x_p is the piston displacement. For each 20−50 attempted chain moves, one piston move is attempted, consisting of a small random displacement of the piston in the neighborhood of its original position. In this move, only the changes in interactions of a chain with the piston wall are evaluated. This simulation approach emulates the nanopiston technique used in experiments to compress DNA molecules in a nanochannel.

RESULTS

Individual Actions of Confinement and Tensile Force.

As a reference, we first compare the separate action of the channel confinement (D) and the external force (f) on DNA molecules. Similarly to tensile external force, confinement of a polymer into a channel is accompanied by its spontaneous stretching. Thus, a DNA molecule brought into a nanochannel typically stretches to about half of its contour length. Both confinement and f constraints reduce the conformational freedom of a molecule: squeezing DNA into a channel or its mechanical deformation from the equilibrium size is accompanied by a free energy penalty. It should be emphasized that the above similarity breaks down for the compressive force $f < 0$, which leads to the chain shortening. Yet, a complementary process of reduction of the longitudinal size of a polymer induced by channel walls is not observed in experiments.

The individual impact of the geometric and tensile constraints on a polymer was earlier explored[2] by the blob scaling theory and MC simulations by assuming sufficiently long polymers chains of pronounced excluded-volume interactions needed for the demarcation of individual scaling regimes in confinement.[13] However, an appropriate assessment of the impact of D and f constraints on DNA requires a comparison over a range of lengths. The single-molecule experiments with DNA often use the molecules of short-to-moderate lengths. The finite-size DNA molecules, such as those assumed in the present simulations, exhibit a large aspect ratio P/w and a weak excluded-volume and thus behave in confinement similarly to the ideal chains.[32,33]

The simulation data for the extensions of DNA molecules in cylindrical channels of the reduced size D/P and at the end-chain stretching by the external force f are shown in Figure 2. The data are presented in the form of the functions $D(R_{II})$ and $f(R_{II})$ to exploit as a common variable the extension R_{II} associated with the polymer experiments in bulk. Since the confinement function $D(R_{II})$ does not involve the chain size reduction, only the stretching branch of the function $f(R_{II})$ is plotted in Figure 2. The reference (unconfined) size of bulk DNA along the x axis is $R_{IIo}/L = 0.12$. The plot of the inverted functions allows visualizing the values of confinement and force needed to attain a given extension R_{II}/L.

The confinement and force functions plotted in Figure 2 show an inverse trend. In the force function $f(R_{II})$, the apparent linear region of entropic elasticity extends up to the fractional extension $R_{II}/L \approx 0.45$. On subsequent stretching of the chain, the internal energy changes (such as the bending energy) intensify, and the restoring force is given as the sum of the energy and entropy components.[34] The dependence of the chain dimensions on channel size $D(R_{II})$ in Figure 2 depicts a well-known increase in the extension of DNA on shrinking of the channel size described in detail by experiments, theory, and simulations.[7,11−13,32,33,35] The specific shape of the function $D(R_{II})$ considerably depends on the DNA contour length. Thus, the function $D(R_{II})$ reported for very long semiflexible

https://dx.doi.org/10.1021/acs.jpcb.9b11602
J. Phys. Chem. B 2020, 124, 1691−1702

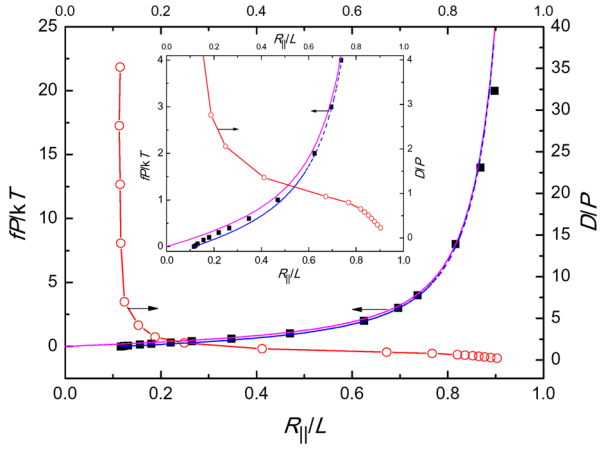

Figure 2. Plots of the reduced force fP/kT (black squares) and the reduced channel width D/P (red circles) against the fractional extension R_{II}/L for a single DNA molecule. Inset: the regions of a weak tensile force and strong-to-moderate confinement. Additionally, the curves according to eq 1 (magenta) and eq 2 (blue) are shown.

polymers in nanochannels[35] covers a much larger span of the extension R_{II}/L and a more steep rise of the D/P values as compared to the data in Figure 2 for the relatively short DNA chains.

Conventionally, the $D(R_{II})$ function in long polymers involves four different confinement regimes.[13] In the Odijk (unfolded) regime of strongly confined polymers at $D < P$, the deflection of stiff polymer segments back and forth from the channel walls results in the substantial chain stretching. Figure 2 shows the onset of this regime at about $D/P \approx R_{II}/L \approx 0.8$. In the backfolded Odijk regime, in channels slightly wider than the above boundary, the wormlike polymer can turn around in the channel and form the hairpin-like structures. Further on, at the transition to moderate confinements, the extended de Gennes regime characterized by anisometric blobs of cylindrical shape is presumed.[13] The fourth, classic de Gennes regime is reached in DNA molecules only in very wide channels ($D \gg P^2/w$).[2,36]

However, not all mentioned confinement regimes are observed in DNA of intermediate (μm) lengths because the chain swelling due to the excluded-volume effects presumed in the scaling theory is relatively weak. The DNA coils occupy a much larger volume than flexible chains of the same length, with fewer collisions between monomers. The channel-induced extension of coils further reduces the self-avoidance effects in DNA at physiological conditions. Hence, due to the weak excluded volume effect in confined DNA, the scaling theory cannot precisely describe the typical channel experiments.[36] As an alternative, a universal theory was developed,[37] which predicts a universal master function for the extension R_{II}/L valid through most of the confinement relevant to DNA experiments.

The data in Figure 2 indicate that the function $D(R_{II})$ is sensitive to the confinement strength primarily below $D/P \approx 3$. For example, a trapping of DNA into the narrow channel $D/P = 0.23$ generates the relative extension $\alpha = R_{II}/R_{IIo} \approx 8$. As an equivalent, the external force about 2.5 pN is needed (Figure 2) to reach such a relative extension by mechanical stretching. Similarly, the *confinement of* $D/P \approx 1$ in micrometer-sized DNA is associated with the relative extension $\alpha = 5.6$. To achieve the same extension through the end-chain stretching, the force $fP/kT \approx 2.39$ (or 0.22 pN) needs to be employed. In contrast, just weak forces of the order of 10−100 fN are sufficient to accomplish the extension equivalent to that occurring at moderate and weak confinements at $D/P > 3$. The shape of the confinement and force functions are slightly modified when the chain displacement in the direction of the x axis is measured by the span S or the arithmetic average $\langle x \rangle$ instead of the quadratic average R_{II} (Figure S1). The average $<x>$ is a preferred quantity in the single-molecule stretching experiments, whereas in experiments with the confined molecules, mostly the span is measured.

The quantitative predictions of the force effect on DNA are far more developed than those for confinement. The force−extension functions in the tensile range are provided both by the WLC and blob theories.[8,9,38] In practice, the stretching response of DNA is most often represented by the MS expression[9] describing the wormlike chains under constant tensile force. Even though f is an independent variable, the MS formula is conventionally presented in the inverted form

$$fP/kT = 0.25\left(1 - \frac{<x>}{L}\right)^{-2} + \frac{<x>}{L} - 0.25 \quad (1)$$

In the development of eq 1, the elastic response at moderate forces was effectively interpolated between the low- and high-force limiting relations. Since the MS formula is universal for a wormlike polymer of a given P and L, eq 1 found widespread use in fitting the stretching data of semiflexible polymers.

The plot in Figure 2 substantiates that the MS relation fits well the R_{II}-based data at moderate and high forces since, in this force range, R_{II} and $<x>$ practically coincide. The deviations in the weak-force region are associated with the fact[10] that eq 1 predicts, at vanishing force, the average displacement $<x>_o = 0$, whereas the corresponding equilibrium quadratic displacement $R_{IIo} = R_o/\sqrt{3}$ is finite at $f = 0$. The modification of the MS relation in the spirit of the proposal in ref 17 is

$$\frac{fP}{kT} = 0.25\left[\frac{1}{(1 - (R_{II}/L))^2} - \frac{1}{(1 - (R_{IIo}/L))^2}\right] + (R_{II}/L) - (R_{IIo}/L) \quad (2)$$

where $<x>$ is replaced by R_{II}, and the term R_{II}/L is reduced by its undeformed value R_{IIo}/L, securing that eq 2 yields the undeformed chain dimensions in the limit of $f = 0$.

In contrast to the WLC model and the quantitative MS relation, the blob model provides only a qualitative assessment of the elastic response of the semiflexible polymers.[38] In this case, a driving force of the blob segregation is the tensile force instead of the self-avoidance of blobs operating in the tube confinement. The diverse elastic regimes from the blob theory are characterized by the scaling relation between the chain displacement and the force. Thus, in the scaling relation $<x> \approx f^y$, the exponent $y = 1$ characterizes the weak-force regime of entropic elasticity, and the exponent $y = 0.7$ characterizes the Pincus regime of the blobs swollen by excluded-volume interactions under moderate forces.[38] The blob model approach was used to compare the geometric and tensile constraints on a swollen polymer.[2] The analysis revealed that, in the de Gennes regime, the effect of confinement on extension is analogous to the effect of the force in the Pincus regime. In contrast, the different scaling functions apply for the

https://dx.doi.org/10.1021/acs.jpcb.9b11602
J. Phys. Chem. B 2020, 124, 1691−1702

chain extension in the extended de Gennes and extended Pincus regime.[2]

As regards the analogy between the functions $D(R_{II})$ and $f(R_{II})$, it is important to note that the quantities f and D are not intrinsically congruent. The external force is related to the elastic free energy of chain stretching $f/kT = d(A_f/kT)/dR$. In contrast, D is a simple geometric measure. Rather than D, the "confinement" force f_D represents a genuine analog to the external force. The thermodynamic quantity f_D is defined in a similar way as the external force f by the derivation of the confinement free energy A_D/kT in a channel $f_D/kT = -d(A_D/kT)/dD$.[3,39] The confinement free energy A_D and force f_D measure the drive of a chain to escape the confined space; $A_D = f_D = 0$ in free space. We have shown that the DNA extension solely by the channel walls ΔR_D requires much higher free energy expenditures than the same extension ΔR_f solely by the external force.[3] The corresponding statement applies to the forces as well: the confinement force $f_D(R_{II})$ attains much larger values in the whole range of DNA extension than the external force $f(R_{II})$ (Figure S2). Such a behavior is mainly a consequence of spatial inequality of confinement and elastic quantities. The confinement quantities A_D and force f_D operate in the transverse direction against the channel walls. An accompanying increase in the longitudinal chain extension ΔR_D is only an indirect outcome of a soft-body squeezing. On the other hand, the elastic quantities act in the direction of the channel axis. Thus, the external force f is perpendicular to the confinement force f_D. As a result, the elastic quantities A_f and f are much more effective in achieving a given longitudinal extension in comparison with the confinement quantities A_D and f_D.

The variance $\sigma_{II}^2 = \langle R_{II}^2 \rangle - \langle x \rangle^2$ computed from simulation data allows us to evaluate the fluctuations around the equilibrium displacement at DNA stretching and confinement. An analogous relation applies to the transversal fluctuations $\sigma_\perp$ in the direction of y and z axes. The plots of the relative fluctuations σ_{II}/L as a function of the constraints D or f in Figure 3 share an existence of the pronounced sharp peak. This apparent similarity of the curves σ_{II}/L is in fact deceptive. Under f constraint, the maximum in σ_{II}/L appears at very weak force $fP/kT \cong 0.6$ (at the low chain extension), and then the σ_{II}/L values rapidly diminish on DNA pulling. As expected, practically unconstrained coils at small forces exhibit, in this case, the largest fluctuations in longitudinal extension. Quite reverse, the maximum in σ_{II}/L is observed in Figure 3 at high extension at $D/P = 0.79$. Here, the large longitudinal fluctuations arise at the onset of the hairpin formation by chain backfolding occurring at strong confinement, that is, at the high extension. Then, the fluctuations rapidly decrease and level-off at weak confinement. The fluctuation maxima in Figure 3 are associated with the points of upturn on the curves $f(R_{II})$ and $D(R_{II})$ in Figure 2. The fluctuation maximum corresponds roughly to the transition of entropy elasticity into the mixed entropy/energy mechanism in the former curve and to the transition to the Odijk regime in the latter curve. On the other hand, the transverse fluctuations $\sigma_\perp/L$ show a consistent behavior in Figure 3: they decrease at the chain extension either due to the force or channel squeezing.

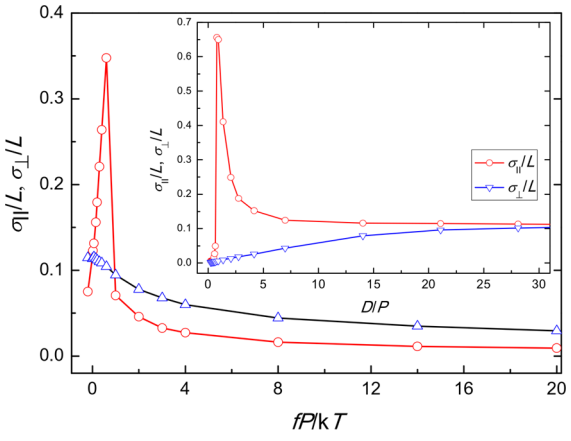

Figure 3. Variations of the relative fluctuations σ_{II}/L (red) and $\sigma_\perp/L$ ((blue) in the longitudinal and transverse direction, respectively, as a function of the reduced force fP/kT and channel size D/P.

End-Chain Stretching and Compression. The DNA molecules confined in a repulsive cylindrical channel and simultaneously subject to the constant longitudinal force are examined by two approaches: end-chain method and piston method. The deformation of molecules in the channel via chain ends allows exploration of the whole function f–R covering the DNA compression and stretching. The present simulations exploit a recent observation[10] that the compression response of DNA can be explored under the constant force when the quadratic average of the displacement is used. Traditionally, the compression behavior of polymers is examined in theory and simulations under the constant length constraint.[3,40,41]

The elastic response of confined DNA at deformation through the chain ends is shown in Figure 4 in the form of $f(R)$ profiles at a given channel size. A distinctive feature of the functions f–R is their shift to the higher displacements on narrowing the channels. Two types of the profiles $f(R)$ can be distinguished in Figure 4 corresponding to (i) weak-to-moderate confinement and (ii) tight confinement. The first

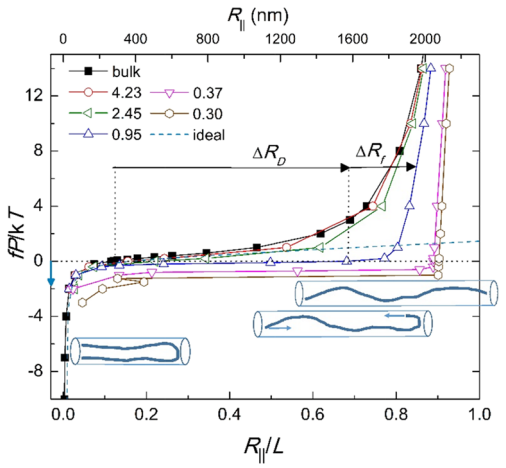

Figure 4. Plots of the reduced force fP/kT at the end-chain deformation against the fractional extension R_{II}/L for a single DNA molecule confined in the channels of the reduced width D/P (4.23 (red), 2.45 (olive), 0.95 (blue), 0.37 (magenta), and 0.30 (brown)) and for bulk DNA (black). The dotted line describes the Gaussian chain behavior in bulk given by eq 3. The interplay of the confinement (ΔR_D) and force (ΔR_f) parts of the displacement is indicated for stretching by force $fP/kT = 7$ in the channel of $D/P = 0.95$. Sketches illustrate the process of compression in the narrow channel. (A zoomed in image to small forces is shown in Figure S3.)

https://dx.doi.org/10.1021/acs.jpcb.9b11602
J. Phys. Chem. B 2020, 124, 1691−1702

type involves the conventional smooth elastic curves for DNA molecules in bulk and in the channels of the intermediate widths. Their displacement points R_{IIo} at $f = 0$ are slightly shifted at moderate confinement to higher R (relative to the bulk). On compression, these curves sharply decrease from their stress-free displacements R_{IIo} at a given D to the ultimate values of R_{II} near zero in the loop-like conformations. Even so, the overall dimensions of a compressed chain at $R_{II} \approx 0$ can still be appreciable due to the finite size of the unstressed components in the y and z directions. The compression branch of the profiles $f(R)$ in Figure 4 is satisfactorily accounted for by the equation

$$fP/kT = 1.5R_{II}/L - 2L/R_{II}t \quad (3)$$

where $t = L/P = 50$, derived in the constant length ensemble for the Gaussian chains in bulk.[10,40] It is widely presumed that the functions $f-R$ are negligibly affected by confinement in wide channels and/or at strong tensile forces. The data in Figure 4 suggest that such insensitivity to confinement also occurs at the moderate and strong compressions by the end-chain deformation mechanism.

In contrast, the second type of profiles $f(R)$ in Figure 4, roughly in the Odijk and backfolded Odijk regimes, shows the shape notably different from the profile in bulk. The functions $f(R)$ for chains considerably pre-stretched by confinement display three distinct regions. In the narrow channels, the curves $f(R)$ steeply raise by strong pulling forces, as expected, due to a substantial tensile stiffening of DNA molecules. In the region of weak compression, a distinct long plateau appears on the curves. At subsequent compression in the last region, the curves $f(R)$ roughly follow eq 3.

Essentially, a sudden collapse of DNA dimensions instead of a gradual compression is predicted by the end-chain deformation method in the narrow channels. The highly extended molecules in the narrow channels are transformed along a quasi-linear part of the functions $f(R)$ into the compact conformations of small R_{II}/L. This abrupt change in the chain displacement at compression can be interpreted by the chain backfolding induced by the external force. In the absence of force, a negligible backfolding is presumed in the Odijk regime in opposition to the backfolded Odijk regime featuring thermally induced hairpins.[13] However, the external force can considerably affect the conventional, "stress-free" boundaries of individual confinement regimes.[3,42] The free energy cost of a hairpin formation in a chain is dictated by the bending energy. The elastic free energy accumulated at the compression by the external force may prevail over the energy barriers even in the Odijk regime and bring about a short turn at the chain ends. Further on, the development of an initial end-turn (the J-shaped hairpin) into a full U-shaped hairpin requires just a small energy and compression force.[43] The fully developed hairpins potentially occurring at strong confinement and strong compression show the end separation $R_{II} \approx 0$, but their span is near half of the contour length $S \cong L/2$. The end-chain deformation mechanism in the narrow channel most likely does not produce the S-type hairpins requiring two bends in the chain interior. The qualitative change in the shape of force−displacement curves arises in Figure 4 at the channel confinement of $D/P = 0.95$. This observation concurs with a very similar value $D/P = 0.9$ assigned in earlier Brownian dynamics simulations[44] to the inception of the hairpins at reduction of the channel width. A detailed comparison of the conformations and dynamics of DNA molecules under strong confinement in channels and slits is elaborated in ref 45.

In a way, the abrupt compression of DNA in narrow channels resembles the buckling instability of a rigid rod under a compressive load. The rod buckles if the compression force exceeds the critical (Euler) force. The buckling by the axial compression is well documented[46−48] for unconfined rigid-rod polymers of $L/P \approx 1$. The stiffness of a DNA molecule of L/P in tens or hundreds is much enhanced on trapping into a narrow channel. It was estimated[49] that the effective persistence length under channel constraints can be one or two orders higher than the inherent value of P and come near to stiffness of the rigid-rod polymers. Consequently, the process occurring in a quasi-linear part of curves in Figure 4 can be pictured as buckling of extended DNA molecules into hairpin conformations.

It is instructive to interpret the functions $f(R)$ in Figure 4 by employing the displacement components due to confinement ΔR_D and force ΔR_f. The displacement points R_{IIo} at $f = 0$ on the $f(R)$ curves are slightly shifted to the right relative to the bulk curve. The corresponding shift due to chain pre-stretching in a given channel, $\Delta R_D = R_{II} - R_{IIo} > 0$, can be attributed solely to the effect of confinement. In a subsequent deformation by force f, the positive or negative extension term ΔR_f is added to the value ΔR_D as illustrated in Figure 4. The relative weight of the above terms depends on the channel size. For example, in a channel of $D/P = 4.23$, the term $\Delta R_D/L = 0.04$, while the term $\Delta R_f/L$ is of the order 0.1, depending on the applied force. On the contrary, in the narrow channel of $D/P = 0.30$, the prevailing confinement term $\Delta R_D/L = 0.78$ is just slightly affected by the term $\Delta R_f/L$. Accordingly, moving from the left to the right in Figure 4, the tensile functions $f(R)$ can be classified as force-dominant or the confinement-dominant. In the compression regime, the positive values ΔR_D in the $f(R)$ functions are combined with the negative terms ΔR_f. As seen from Figure 4, only minor negative forces are needed to attain such a value of ΔR_f that fully compensates the wall-induced pre-stretching of DNA.

The variability of the $f-R$ functions according to the channel size observed in Figure 4 agrees with the similar observations for DNA in nanoslits at 2d confinement. The tensile curves $f(R)$ in slits are shifted to the right relative to bulk in the same way as in Figure 4.[16−18] Obviously, the confinement term ΔR_D in slits is much smaller than in channels. Since a given force produces a larger chain extension in slits and channels than in bulk, such a behavior formally suggests an apparent "elastic softening" of a DNA in quasi-1d and quasi-2d confinements. In fact, the shift of the $f-R$ functions both in slits and channels is primarily brought by the confinement-induced chain extension ΔR_D. Figure 4 confirms that the actual molecular stiffness associated with the term ΔR_f increases on the tightening of confinement.

The elastic response of DNA confined in channels shown in Figure 4 is not reproduced by the current theories of semiflexible chains. For unconfined chains, several analytical $f-R$ relations originating mostly from the WLC model are available.[48] The popular MS formula, eq 1, provides the prediction only for the tension regime. An alternative equation $f-R$ from the Blundell−Terentjev model[48] covers both the tension and compression/buckling regimes. In an attempt to semi-empirically adapt the MS formula to the confined systems, we first exploited eq 2. A reduction of the extension R_{II}/L by its undeformed value R_{IIo}/L offered by eq 2 plays an

https://dx.doi.org/10.1021/acs.jpcb.9b11602
J. Phys. Chem. B 2020, 124, 1691−1702

essential role in Figure 4. The individual tensile functions $f(R)$ were fitted by eq 2 by using the stress-free displacements R_{IIo} at a given channel size. The fit of data is acceptable at the week and strong confinements (Figure S4). However, eq 2 fails in the prediction of the shape of the $f(R_{II})$ functions at the intermediate channel widths.

In another alternative, an approach to the $f-R$ function of wormlike chains in narrow slits used in ref 17 was applied to the channels. The persistence length P in eq 2 is replaced in confinement by the segmental correlation length P_{II} measuring the chain stiffness in the longitudinal (unconfined) dimension. In slits, the $f-R$ functions computed for variable slit widths collapsed onto a single master curve when plotted by using eq 2 in which the leftmost term was amended to fP_{II}/kT.[17] In the application of this approach to channels, the terms P_{II} and $P_{\perp}$ expressing the correlation lengths in DNA chains in the axial and transverse directions[31] were employed. In contrast to the slits, where the ratio of P_{II}/P saturates to a maximum at P_{II}/P = 2 on narrowing the slits,[17] in narrow channels, this ratio attains the values higher by the two orders of magnitude (Figure S5). Consequently, the whole procedure is of insufficient merit for channels since the resulting master curve $f-R$ involves just a successive head-to-tail superposition of the individual functions for given D (Figure S5).

Finally, the end-chain fluctuations when D and f constraints act simultaneously are judged against the case of their separate actions. The fluctuations σ_{II} of a confined DNA molecule deformed through the chain ends shown in Figure 5 are closely

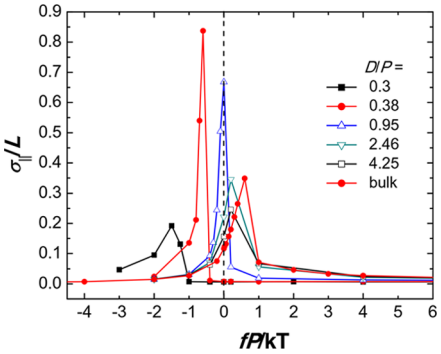

Figure 5. Fluctuations versus force for different confinement ratios D/P indicated in the legend.

associated with the transitions in the $f-R$ curves in Figure 4. The maxima in the function σ_{II} plotted against the force in Figure 5 coincides with the plateau region in Figure 4, where a small change of force leads to the large changes in the chain displacement. On narrowing the channels, the maximum of fluctuations shifts from the tensile forces to the compressive regime. Interestingly, for D/P = 0.95, close to the onset of the Odijk regime, the fluctuations maximize at fP/kT = 0. A similar maximum of fluctuations was found in slit-like channels at the transition between moderate and strong confinement.[50]

Piston Compression. The compression of DNA by a sliding piston in a cylinder is monitored in simulations by the span S. Since S is the longest dimension of a polymer along the channel x axis, the identity $S \equiv S_{II}$ applies. In bulk DNA the equilibrium span S_o/L = 0.16 is slightly larger than longitudinal end-to-end dimensions R_{IIo}/L = 0.12. Such a correlation is valid as well in channels: the spans S_{oD}/L at f = 0 for a given D are always slightly higher than the corresponding values R_{IIoD}/L (Figure S1).

The forces up to 0.9 pN were employed in piston compression simulation of DNA (Figure 6). The piston

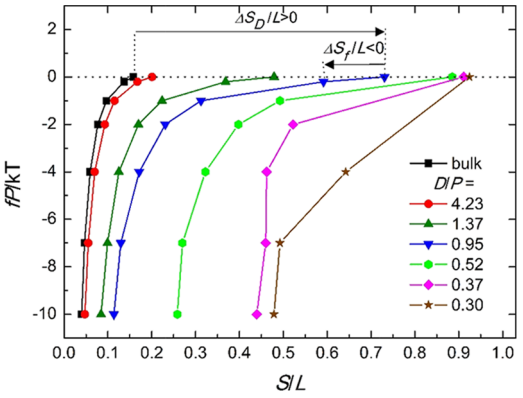

Figure 6. Plots of the reduced force fP/kT at piston compression against the fractional span S/L for a single DNA molecule confined in the channels of the reduced width D/P (4.23 (red), 1.37 (olive), 0.95 (blue), 0.52 (green), 0.37 (magenta), and 0.30 (brown)) and for bulk DNA (black). The interplay of the positive term $\Delta S_D/L$ due to confinement pre-stretching and the negative term $\Delta S_f/L$ due to compression by the external force is illustrated for the channel of D/P = 0.95.

compression curve $f(S)$ for bulk DNA is quite similar to the corresponding end-chain function $f(R_{II})$ in Figure 4. On the other hand, in channels, the piston functions $f(S)$ in Figure 6 are, in many respects, at variance with those obtained by the end-chain mechanism. Primarily, a smooth compression response of DNA is observed in the piston case in Figure 6 in the whole range of the channel sizes. Furthermore, in contrast to the end-chain mechanism, each channel size in Figure 6 is characterized by a specific compression curve. The piston functions $f(S)$ shows two distinct regions: the region of slow compression at weak negative forces followed by an abrupt decrease in displacement at stronger forces. A resolution of the overall span into the ΔS_D and ΔS_f parts in Figure 6 shows that, in case of compression, the negative force term ΔS_f is acting in opposition to the positive confinement term ΔS_D. In narrow channels, the chain pre-stretching induced by confinement is so large ($\Delta S_D/L$ = 0.76 at D/P = 0.30) that even at the strong compression forces the chain shortening due to ΔS_f is not large enough to offset the confinement pre-stretching ΔS_D.

The piston curves $f(S)$ shown in Figure 6 can be viewed as a gradual compaction of a DNA molecule on compression. At f = 0 and weak-to-moderate confinements (roughly above D/P = 1), the confined molecules are presumed to exist in a disordered state portrayed as a melt of blobs akin to the semidilute solution.[27] On compression, the molecule tends to reach compact, quasi-globular conformations of small S values seen in Figure 6. The degree of DNA compaction can be roughly estimated at weak confinement. Although in wide channels the isotropic bulk state at f = 0 is perturbed, the longitudinal and transverse dimensions of a DNA coil could still be fairly similar and amount to $S_o \approx R_{IIo} \approx R_{\perp o} \approx$ 300 nm (Figure 6). The compression of confined molecules in wide channels by the force fP/kT = −10 changes their longitudinal dimension to $R_{II} \approx$ 100 nm (Figure 6). Hence, the pervaded

https://dx.doi.org/10.1021/acs.jpcb.9b11602
J. Phys. Chem. B 2020, 124, 1691−1702

volume of a DNA molecule is reduced to about one-third of the initial volume at $f = 0$, provided that the transverse dimensions do not change in this compression process.

In narrow channels, the DNA compaction at the piston compression also includes the folding of DNA molecules in the middle of a chain into the *S*-type hairpins. This phenomenon can give an explanation to sizeable spans S that persist in Figure 6 even at strong compressive forces at tight confinements, presumably in the Odijk and backfolded Odijk regimes. For example, DNA compression in the channel of $D/P = 0.30$ yields the span $S/L \approx 0.5$ at $fP/kT = -10$. Incidentally, the same span characterizes the simple U-turn hairpin for which a relation $S \cong L/2$ applies. The radial distribution function $P(R)$ serves as a useful indicator of the formation of hairpins and their clusters in DNA chains confined in narrow channels.[51,52] The related functions $P(S)$ for DNA in the channel of $D/P = 0.52$ presented in Figure S6 suggest a fairly uniform conformation of DNA in the stress-free state. However, the functions $P(S)$ under negative forces provide clear evidence that a range of the J- and U-shaped hairpins arise in confined DNA molecules on compression (Figure S6). The formation of hairpins on DNA compression in the Odijk regime is supported by the recent Brownian dynamics simulations of strongly confined DNA in square channels that revealed the series of chain folding events accompanying non-equilibrium piston compression.[27] The simulation[27] predicts the emergence of the organized compressed state of DNA by the repeated nucleation events and growth of nested hairpin structures.

The response of DNA molecules in channels to the external compression force can be characterized by the function $\chi = -(1/S)(\mathrm{d}S/\mathrm{d}|f|)$ defining the compressibility of DNA in a cylinder by a piston in an analogy with the conventional isothermal compressibility. Figure S7 shows that the DNA compressibility is at maximum for weak forces and progressively diminish by stronger forces where the chain compacting at closed contacts the DNA segments mutually and that with the channel walls becomes more difficult. Contra-intuitively, the stretched molecules in the narrow channels are most malleable and show the highest χ in the first stages of compression.

The piston compression was earlier explored by the scaling theory and molecular simulations of a flexible, self-avoiding chain in a cylinder.[21] The analytical theory based on Flory-type expression of the free energy was used to formulate the dependence of the force on the channel size

$$\frac{fP}{kT} = \frac{KP}{D}\left(\left(\frac{R}{R_o}\right) - \left(\frac{R_o}{R}\right)^2\right) \quad (4)$$

where K is dimensionless polymer spring constant. The first term in brackets describes the elastic entropy of a polymer made of blobs, and the second term describes the mutual exclusion between neighboring blobs. Equation 4 envisages a universal scaling relation for the compression and tensile deformation of a self-avoiding chain in a cylinder on assumptions that it can be represented as a linear string of blobs and at deformation and behaves as an entropic spring. In recent simulations,[23] the piston compression function $f(R)$ for DNA in the channel size of about $D/P = 2$ in our notation corroborated the reliability of eq 4. The function $f(R)$ from ref 23 shows a close resemblance to the respective curve $f(S)$ in Figure 6, displaying at first the fairly effortless compression regime followed by the region of the strenuous compression.

Following the original approach for excluded-volume chains,[21] we replicated the analysis for the pseudoideal chains of the weak excluded volume, such as in confined DNA, where $R \approx N^{0.5}$. The $f(R)$ function resulting from such analysis retains the form of eq 4. Hence, the piston compression curves $f(S)$ in Figure 6 allow testing the validity of eq 4 for a wide scale of channel sizes. In harmony with eq 4, the plots $f(\alpha)$ are presented in Figure 7, where the coefficient $\alpha = S/S_{oD}$ gives the

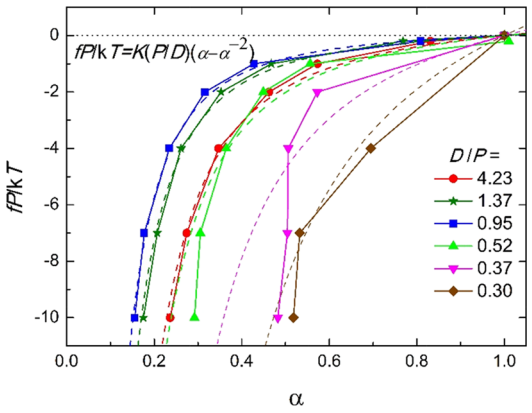

Figure 7. Comparison of the dependence of the reduced force fP/kT at piston compression of confined DNA against the coefficient $\alpha = S/S_{oD}$ from our simulations (symbols) and from eq 4 based on the blob theory (dashed lines) for the channel widths D/P: 4.23 (red), 1.37 (olive), 0.95 (blue), 0.52 (green), 0.37 (magenta), and 0.30 (brown).

change of the span of DNA molecules on compression relative to the stress-free span S_{oD} at a given D. Figure 7 shows that eq 4 reasonably well represents the force profiles $f(\alpha)$ from simulations in the channels of $D/P \approx 1$ and larger, provided the effective spring constant K is individually fitted for every profile $f(S)$. In narrow channels, the blob compression stipulation underlying eq 4 fails because of the hairpin formation. Moreover, the order of curves in Figure 7 with respect to the channel size suggests a nonmonotonous dependence of the spring constant K on D that contradicts the prediction $k \approx D^{-0.33}$ implying from eq 4.[21]

The plotting of the polymer size as a function of the channel width in the logarithm scale is an established practice in the scaling theory of confined polymers in the absence of the external force.[13] Thus, the piston compression data are recast in Figure 8 into the plot of the fractional span S/L as a function of D/P for the various compression forces (in the absolute value). The uppermost curve in Figure 8 describes the conventional confinement behavior at $|f| = 0$. The remaining curves correspond to a gradual transfer of a DNA molecule compressed by a given force into the narrower channels. In DNA molecules, the large contour lengths are needed to explore the distinctive power laws in the individual confinement regimes.[2,36] For the finite-size DNA molecules, only short quasi-linear sections are present in the middle of the logarithmic plots $S(D)$ (Figure 8). From the limited data set, just a qualitative observation of a similarity in the shape of the curves in Figure 8 can be drawn. Some effect of the piston compression force on the confinement regimes is seen only in narrow channels. The Odijk regime, distinctive at $|f| = 0$ in Figure 8, fails to materialize at the high compressive forces.

https://dx.doi.org/10.1021/acs.jpcb.9b11602
J. Phys. Chem. B 2020, 124, 1691−1702

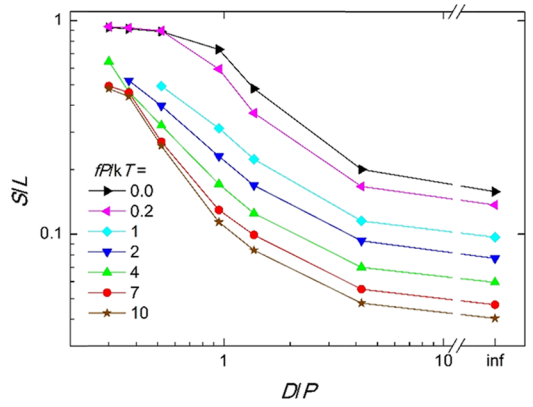

Figure 8. Fractional span of DNA as a function of reduced channel width at piston compression forces (in the absolute value) given in the legend.

An alternative presentation of the combined effect of D and f constraints on DNA provides the scaling plot of the span S versus the piston compression force $|f|$ at various channel sizes (Figure 9). Unlike the tensile forces,[2,38] the scaling analysis of

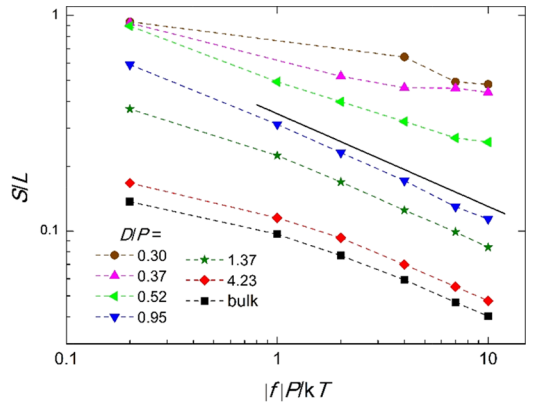

Figure 9. Fractional span of DNA as a function of at the reduced piston compression forces (in the absolute value) at channel size D/P given in the legend. The full (scaling) line is explained in the text.

polymers under the external compressive forces is not yet elaborated. In the majority of channel sizes, the $S(f)$ curves in Figure 9 show the quasi-linear section in the range of forces $|f|P/kT > 1$ that can be accounted for by the power-law function $S \approx |f|^{y}$. The exponent y is related to the spring constant K, and its value in Figure 9 slightly varies at intermediate and weak confinements where the blob-model picture of DNA compression may apply. The exponent $y = -0.43$ shown in Figure 9 by a solid line well agrees with the exponent $Y = 1/y = -2.25$ in the inverse relation $|f| \approx R^{Y}$ obtained from the compression simulations of flexible chains.[21]

DISCUSSION

We have shown that the tensile elasticity of DNA molecules confined in channels follows a characteristic pattern (Figure 4) involving the shift of $f-R$ functions to the larger extension relative to the bulk. This shift, observed also in slits,[16−18] is a consequence of DNA pre-stretching under confinement expressed by the term ΔR_D. Once this shift is eliminated, the elastic curves $f-R$ show the slopes rising proportionally to the effective stiffening of DNA at narrowing the channels (Figure S8), as predicted by the WLC model of unconfined semiflexible polymers.

The force−displacement relations in the compressive regime of confined DNA are more complex. The compressive response offered by the end-chain and the piston methods can be sorted out into two types. In the first type, at weak and moderate confinements, a comparable compression behavior of confined DNA is offered by both methods. The compression curves $f-R$ from the end-chain method in Figure 4 can be well approximated by eq 3 for ideal chains. Similarly, eq 4 provides a reasonable approximation of the $f-S$ curves in Figure 6 from the piston method. In both cases, a mechanism of gradual compaction of disordered blob-melt DNA molecules can be presumed.

The second type of compression response is associated with the emergence of hairpin-like structures in DNA molecules in narrow channels. However, two deformation mechanisms provide contrasting elastic curves at tight confinement. In the piston compression mechanism the formation of hairpins in narrow channels is depicted by a continuous course of the $f-S$ functions (Figure 6). On the contrary, the $f-R$ curves from the end-chain method exhibit an abrupt (buckling) transition from the extended to hairpin conformations at small compressive forces (Figure 4). Since the effective stiffness of DNA molecules is much enhanced in narrow channels, small compressive forces at the end-chain deformation are sufficient to induce DNA buckling. The linking of a plateau on the $f-R$ curves in Figure 4 to chain buckling is supported by the data for unconfined polymers. The studies based on the analytical model[48] or MC simulations[53] confirmed the existence of a buckling plateau on the $f-R$ curves at the compression of stiff unconfined polymers. The compression of very stiff short DNA molecules at tight confinements may in an extreme case bring about the buckling of the deflection segments and the formation of a helix.[54]

This discrepancy between the compressive functions $f-R$ in Figure 4 and the $f-S$ functions in Figure 6 is linked to the nature of the two quantities R_{II} and S used to measure the displacement in two methods. In the piston method, the compressive force is transmitted through the contacts of the farthermost distant (usually intra-chain) segments with the barrier walls. Various techniques involving movable pistons, beads, and funnels were designed to compress DNA molecules in nanochannels.[6,24−28] In such experiments, the span S is usually determined through the optical imagining of stained DNA molecules. On the other hand, in the end-chain method, the compression force acting at the chain ends diminishes the separation R_{II} in the direction to the loop-like conformations. The end-to-end distance R and its component R_{II} are central variables in the polymer elasticity theories.[1] The design of compression experiments with single polymers involving the variable R_{II} could be complicated. Often, an analogy between the external force in single-chain deformation and the Coulomb interaction of the charges located on the chain ends is brought into consideration. In the case of a chain carrying the opposite charges, their attraction could imitate the compression force.

It is instructive to compare the development of the extension R_{II} and span S at compression by each of the two methods. As illustrated in Figure 10 for $D/P = 0.95$, the displacement R_{II} computed at the end-chain deformation tends to small values in loop-like conformations; the dimensions along the y and z axes may remain unaffected in the process. The quantity R_{II}

https://dx.doi.org/10.1021/acs.jpcb.9b11602
J. Phys. Chem. B 2020, 124, 1691−1702

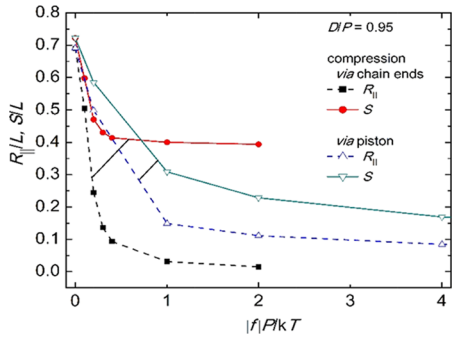

Figure 10. Comparison of two compression modes and their effect on R_{II} and S for D/P = 0.95.

from the piston method simulations shows a similar dependence (Figure 10) but requires higher forces to reach a given value than in the case of the end-chain method. Moreover, both methods demonstrated in Figure 10 that the span S, measuring global compaction of a chain at compression, is much higher than the corresponding value of R_{II}. In other words, the DNA compression by the piston method requires stronger forces to reach a given displacement that the end-chain method. In addition, the span slowly converges from the moderate values to a finite nonzero value, in a difference to R_{II} that the limit approaches $R_{II} = 0$. The described behavior of the variables R_{II} and S explains why the chain backfolding, widespread at tight confinement, is differently exposed in two compression mechanisms in Figures 4 and 6.

Compression of DNA in channels gained recently a good deal of attention because of its association with the self-entanglement and knotting of DNA chains.[24,28,55] The knot formation in DNA is of particular significance because of a high degree of compaction experienced by packed genomes. The nanofluidic systems are employed to produce an enhanced population of DNA molecules with simple knots tied in.[28] The chain compaction induced by confinement or compression significantly enhances the knotting probability relative to the one in the uncompressed bulk state. Sufficiently deep looping and backfolding of the chains ends is crucial for the formation of self-entanglement and knots.[55] The extensive knotting of DNA found in simulations and experiments at weak-to-moderate confinement was related[31] to a powerful looping of DNA chain perpendicularly to the channel walls. The loops must be threaded by one of the chain ends to create a knot. Consequently, one may suppose that the chain-end compression method should be more effective than the piston method in the induction of DNA knotting in nanochannels.

CONCLUSIONS

We have demonstrated that the simulations can provide useful insights into the elastic properties of DNA under the combined action of force and confinement. As a novelty, our analysis presents an integrated description of the force−displacement functions for both the tensile and compression regimes of DNA in the range from 3d to quasi-1d space. Moreover, the simulation data provide an elucidation of the deformation mechanism of DNA by the sliding nanopiston method popular in compression experiments[6,26−28] in nanochannels.

In the tensile regime, the functions $f-R$ are critically affected by the DNA pre-stretching in a given channel that is quantified by the confinement term ΔR_D. In the force-dominant regime at weak-to-moderate confinement, the term ΔR_D is small and the $f-R$ functions resemble that for the bulk DNA. However, in the confinement-dominant regime of large ΔR_D, the $f-R$ functions after the elimination of pre-stretching match those for the stiff rod-like polymers.

In the compressive regime, the response of confined DNA much depends on the deformation mechanism. When the compressive force acts through chain ends, a gradual compression is seen in the $f-R$ curves in wide and intermediary channels. However, in narrow channels, the $f-R$ functions feature a distinct long plateau indicating an abrupt collapse of DNA dimensions. This phenomenon, occurring at weak compression, is interpreted as a buckling instability due to the formation of the hairpin-like structures in the Odijk and backfolded Odijk regimes. The potential advantage of the end-chain compression mechanism for the self-entanglement and knotting of DNA chains are pointed out.

In the second, sliding piston mechanism of DNA compression, the span S is employed to register the DNA compression. Unexpectedly, the smooth compression curves $f-S$ are observed in the whole range of the channel sizes, even though the formation of DNA hairpins on compression in narrow channels was as well demonstrated in this mechanism. This discrepancy between the compression response of DNA provided by the functions $f-R$ and $f-S$ is associated with the nature of two measures of the chain displacement, R_{II} and S. In general, the span S measuring global compaction of a chain exhibits at compression much higher values than the corresponding end-chain separation R_{II} tending to zero in loop-like conformations. Consequently, the chain backfolding, widespread at tight confinement, is differently manifested in the two compression functions $f-R$ and $f-S$. Overall, we expect that a united description of the elasticity of single DNA molecules in the tensile and compressive regimes will prove useful in the understanding of complex DNA behavior in arrays of channels in the micro/nanofluidic devices and in crowded cell environments.

ASSOCIATED CONTENT

Supporting Information

The Supporting Information is available free of charge at https://pubs.acs.org/doi/10.1021/acs.jpcb.9b11602.

(Figures S1−S8) Details on DNA response to the combined effect of confinement and force (PDF)

AUTHOR INFORMATION

Corresponding Author

Peter Cifra − *Polymer Institute, Slovak Academy of Sciences 84541 Bratislava, Slovakia;* orcid.org/0000-0003-2075-4179; Email: cifra@savba.sk

Author

Tomáš Bleha − *Polymer Institute, Slovak Academy of Sciences 84541 Bratislava, Slovakia*

Complete contact information is available at: https://pubs.acs.org/10.1021/acs.jpcb.9b11602

Notes

The authors declare no competing financial interest.

■ ACKNOWLEDGMENTS

This work was supported by grants SRDA-15-0323 and VEGA 2/0055/16. Furthermore, the authors would like to acknowledge the contribution of the COST Action CA17139.

■ REFERENCES

(1) Grosberg, A. Y.; Khokhlov, A. R. *Statistical Physics of Macromolecules*; American Institute of Physics ed.; New York, 1st edn., 1994.
(2) Dai, L.; Doyle, P. S. Comparisons of a Polymer in Confinement Versus Applied Force. *Macromolecules* **2013**, *46*, 6336−6344.
(3) Bleha, T.; Cifra, P. Stretching and Compression of DNA by External Forces under Nanochannel Confinement. *Soft Matter* **2018**, *14*, 1247−1259.
(4) Neuman, K. C.; Nagy, A. Single-Molecule Force Spectroscopy: Optical Tweezers Magnetic Tweezers and Atomic Force Microscopy. *Nat. Methods* **2008**, *5*, 491.
(5) Kriegel, F.; Ermann, N.; Lipfert, J. Probing the Mechanical Properties, Conformational Changes, and Interactions of Nucleic Acids with Magnetic TweezSers. *J. Struct. Biol.* **2017**, *197*, 26−36.
(6) Reccius, C. H.; Mannion, J. T.; Cross, J. D.; Craighead, H. G. Compression and Free Expansion of Single DNA Molecules in Nanochannels. *Phys. Rev. Lett.* **2005**, *95*, 268101.
(7) Reisner, W.; Larsen, N. B.; Flyvbjerg, H.; Tegenfeldt, J. O.; Kristensen, A. Directed Self-Organization of Single DNA Molecules in a Nanoslit Via Embedded Nanopit Arrays. *Proc. Natl. Acad. Sci. U. S. A.* **2009**, *106*, 79−84.
(8) Bustamante, C.; Smith, S. B.; Liphardt, J.; Smith, D. Single-Molecule Studies of DNA Mechanics. *Curr. Opin. Struct. Biol.* **2000**, *10*, 279−285.
(9) Marko, J. F.; Siggia, E. D. Stretching Dna. *Macromolecules* **1995**, *28*, 8759−8770.
(10) Bleha, T.; Cifra, P. Force-Displacement Relations at Compression of Dsdna Macromolecules. *J. Chem. Phys.* **2019**, *151*, No. 014901.
(11) Daoud, M.; De Gennes, P.-G. Statistics of Macromolecular Solutions Trapped in Small Pores. *J. Phys. (Paris)* **1977**, *38*, 85−93.
(12) Odijk, T. On the Statistics and Dynamics of Confined or Entangled Polymers. *Macromolecules* **1983**, *16*, 1340−1344.
(13) Dai, L.; Renner, C. B.; Doyle, P. S. The Polymer Physics of Single DNA Confined in Nanochannels. *Adv. Colloid Interface Sci.* **2016**, *232*, 80−100.
(14) Taloni, A.; Yeh, J.-W.; Chou, C.-F. Scaling Theory of Stretched Polymers in Nanoslits. *Macromolecules* **2013**, *46*, 7989−8002.
(15) Li, X.; Dorfman, K. D. Effect of Excluded Volume on the Force-Extension of Wormlike Chains in Slit Confinement. *J. Chem. Phys.* **2016**, *144*, 104902.
(16) Yeh, J.-W.; Szeto, K. Stretching of Tethered DNA in Nanoslits. *ACS Macro Lett.* **2016**, *5*, 1114−1118.
(17) Chen, Y.-L.; Lin, P.-k.; Chou, C.-F. Generalized Force−Extension Relation for Wormlike Chains in Slit Confinement. *Macromolecules* **2010**, *43*, 10204−10207.
(18) de Haan, H. W.; Shendruk, T. N. Force−Extension for DNA in a Nanoslit: Mapping between the 3d and 2d Limits. *ACS Macro Lett.* **2015**, *4*, 632−635.
(19) Wang, J.; Gao, H. Stretching a Stiff Polymer in a Tube. *J. Mater. Sci.* **2007**, *42*, 8838−8843.
(20) Li, R.; Wang, J. Stretching a Semiflexible Polymer in a Tube. *Polymer* **2016**, *8*, 328.
(21) Jun, S.; Thirumalai, D.; Ha, B.-Y. Compression and Stretching of a Self-Avoiding Chain in Cylindrical Nanopores. *Phys. Rev. Lett.* **2008**, *101*, 138101.
(22) Jung, Y.; Jun, S.; Ha, B.-Y. Self-Avoiding Polymer Trapped inside a Cylindrical Pore: Flory Free Energy and Unexpected Dynamics. *Phys. Rev. E* **2009**, *79*, No. 061912.
(23) Pereira, M. C. F.; Brackley, C. A.; Lintuvuori, J. S.; Marenduzzo, D.; Orlandini, E. Entropic Elasticity and Dynamics of the Bacterial Chromosome: A Simulation Study. *J. Chem. Phys.* **2017**, *147*, No. 044908.
(24) Tang, J.; Du, N.; Doyle, P. S. Compression and Self-Entanglement of Single DNA Molecules under Uniform Electric Field. *Proc. Natl. Acad. Sci. U. S. A.* **2011**, *108*, 16153−16158.
(25) Zhou, J.; Wang, Y.; Menard, L. D.; Panyukov, S.; Rubinstein, M.; Ramsey, J. M. Enhanced Nanochannel Translocation and Localization of Genomic DNA Molecules Using Three-Dimensional Nanofunnels. *Nat. Commun.* **2017**, *8*, 807.
(26) Khorshid, A.; Zimny, P.; Tétreault-La Roche, D.; Massarelli, G.; Sakaue, T.; Reisner, W. Dynamic Compression of Single Nanochannel Confined DNA Via a Nanodozer Assay. *Phys. Rev. Lett.* **2014**, *113*, 268104.
(27) Bernier, S.; Huang, A.; Reisner, W.; Bhattacharya, A. Evolution of Nested Folding States in Compression of a Strongly Confined Semiflexible Chain. *Macromolecules* **2018**, *51*, 4012−4022.
(28) Amin, S.; Khorshid, A.; Zeng, L.; Zimny, P.; Reisner, W. A Nanofluidic Knot Factory Based on Compression of Single DNA in Nanochannels. *Nat. Commun.* **2018**, *9*, 1506.
(29) Cifra, P. Channel Confinement of Flexible and Semiflexible Macromolecules. *J. Chem. Phys.* **2009**, *131*, 224903.
(30) Benková, Z.; Námer, P.; Cifra, P. Stripe to Slab Confinement for the Linearization of Macromolecules in Nanochannels. *Soft Matter* **2015**, *11*, 2279−2289.
(31) Bleha, T.; Cifra, P. Correlation Anisotropy and Stiffness of DNA Molecules Confined in Nanochannels. *J. Chem. Phys.* **2018**, *149*, No. 054903.
(32) Cifra, P.; Benková, Z.; Bleha, T. Chain Extension of DNA Confined in Channels. *J. Phys. Chem. B* **2009**, *113*, 1843−1851.
(33) Wang, Y.; Tree, D. R.; Dorfman, K. D. Simulation of DNA Extension in Nanochannels. *Macromolecules* **2011**, *44*, 6594−6604.
(34) Cifra, P.; Bleha, T. Force−Extension Relations in Macromolecules of Variable Excluded Volume and Flexibility: Energy and Entropy Changes on Stretching. *J. Chem. Soc., Faraday Trans.* **1995**, *91*, 2465−2471.
(35) Tree, D. R.; Wang, Y.; Dorfman, K. D. Extension of DNA in a Nanochannel as a Rod-to-Coil Transition. *Phys. Rev. Lett.* **2013**, *110*, 208103.
(36) Bhandari, A. B.; Dorfman, K. D. Simulations Corroborate Telegraph Model Predictions for the Extension Distributions of Nanochannel Confined DNA. *Biomicrofluidics* **2019**, *13*, No. 044110.
(37) Werner, E.; Cheong, G. K.; Gupta, D.; Dorfman, K. D.; Mehlig, B. One-Parameter Scaling Theory for DNA Extension in a Nanochannel. *Phys. Rev. Lett.* **2017**, *119*, 268102.
(38) Saleh, O. A. Perspective: Single Polymer Mechanics across the Force Regimes. *J. Chem. Phys.* **2015**, *143*, 194902.
(39) Bleha, T.; Cifra, P. Polymer-Induced Depletion Interaction between Weakly Attractive Plates. *Langmuir* **2004**, *20*, 764−770.
(40) Neumann, R. M. On the Precise Meaning of Extension in the Interpretation of Polymer-Chain Stretching Experiments. *Biophys. J.* **2003**, *85*, 3418−3420.
(41) Hyeon, C.; Dima, R. I.; Thirumalai, D. Size, Shape, and Flexibility of Rna Structures. *J. Chem. Phys.* **2006**, *125*, 194905.
(42) Su, T.; Purohit, P. K. Entropically Driven Motion of Polymers in Nonuniform Nanochannels. *Phys. Rev. E* **2011**, *83*, No. 061906.
(43) Polson, J. M.; Tremblett, A. F.; McLure, Z. R. N. Free Energy of a Folded Polymer under Cylindrical Confinement. *Macromolecules* **2017**, *50*, 9515−9524.
(44) Chen, Y.-L. Electro-Entropic Excluded Volume Effects on DNA Looping and Relaxation in Nanochannels. *Biomicrofluidics* **2013**, *7*, No. 054119.
(45) Chen, Y.-L.; Lin, Y.-H.; Chang, J.-F.; Lin, P.-k. Dynamics and Conformation of Semiflexible Polymers in Strong Quasi-1d and -2d Confinement. *Macromolecules* **2014**, *47*, 1199−1205.
(46) Palenčár, P.; Bleha, T. Bending and Kinking in Helical Polymers. *J. Polym. Sci., Part B: Polym Phys.* **2015**, *53*, 1345−1357.
(47) Kurzthaler, C.; Franosch, T. Exact Solution for the Force-Extension Relation of a Semiflexible Polymer under Compression. *Phys. Rev. E* **2017**, *95*, No. 052501.

https://dx.doi.org/10.1021/acs.jpcb.9b11602
J. Phys. Chem. B 2020, 124, 1691−1702

(48) Meng, F.; Terentjev, E. M. Theory of Semiflexible Filaments and Networks. *Polymer* **2017**, *9*, 52.
(49) Cifra, P.; Benková, Z.; Bleha, T. Persistence Length of DNA Molecules Confined in Nanochannels. *Phys. Chem. Chem. Phys.* **2010**, *12*, 8934−8942.
(50) Huang, A.; Bhattacharya, A. DNA Confined in a Two-Dimensional Strip Geometry. *Europhys. Lett.* **2014**, *106*, 18004.
(51) Cifra, P.; Bleha, T. Shape Transition of Semi-Flexible Macromolecules Confined in Channel and Cavity. *Eur. Phys. J. E: Soft Matter Biol. Phys.* **2010**, *32*, 273−279.
(52) Cifra, P.; Bleha, T. Detection of Chain Backfolding in Simulation of DNA in Nanofluidic Channels. *Soft Matter* **2012**, *8*, 9022−9028.
(53) Cifra, P.; Bleha, T. Free Energy of Deformation of the Radius of Gyration in Semiflexible Chains. *Macromol. Theory Simul.* **2007**, *16*, 501−512.
(54) Hayase, Y.; Sakaue, T.; Nakanishi, H. Compressive Response and Helix Formation of a Semiflexible Polymer Confined in a Nanochannel. *Phys. Rev. E* **2017**, *95*, No. 052502.
(55) Micheletti, C.; Orlandini, E. Knotting and Unknotting Dynamics of DNA Strands in Nanochannels. *ACS Macro Lett.* **2014**, *3*, 876−880.

https://dx.doi.org/10.1021/acs.jpcb.9b11602
J. Phys. Chem. B 2020, 124, 1691−1702